Cardiac Malformations Are Associated with Altered Expression of Vascular Endothelial Growth Factor and Endothelial Nitric Oxide Synthase Genes in Embryos of Diabetic Mice

SRINIVASAN DINESH KUMAR, SOOK-KWIN YONG, S. THAMEEM DHEEN, BOON-HUAT BAY, AND SAMUEL SAM-WAH TAY[1]

Department of Anatomy, Yong Loo Lin School of Medicine, National University Health System, National University of Singapore, Singapore 117597

The aim of this study was to investigate the role of nitric oxide (NO), and the expression of endothelial nitric oxide synthase (eNOS) and vascular endothelial growth factor (VEGF) genes in developing hearts at embryonic day 13.5 of embryos from diabetic mice. The protein and mRNA expression levels of eNOS and VEGF were significantly altered in the developing hearts of embryos from diabetic mice. The NO level was significantly decreased, whereas the VEGF concentration was significantly increased in the developing hearts of the embryos from diabetic mice. *In vitro* study showed a significant reduction in eNOS expression and cell proliferation in cardiac myoblast cells exposed to high glucose concentrations. Further, high glucose induced apoptosis in myoblast cells. Ultrastructural changes characteristics of apoptosis, including cell blebbing, aggregation of ribosomes and vacuoles in the cytoplasm were also evident in myoblast cells exposed to high glucose. It is suggested that hyperglycemia alters the expression of eNOS and VEGF genes that are involved in the regulation of cell growth and vasculogenesis, thereby contributing to the cardiac malformations seen in embryos from diabetic mice. Exp Biol Med 233:1421–1432, 2008

Key words: maternal diabetes; developing heart; H9C2 cell line; VEGF; eNOS; mice

Introduction

Diabetes mellitus is associated with an increased risk for congenital malformations which are the major causes for mortality and morbidity in the offspring of diabetic pregnancy (1–4). The congenital malformations in diabetic pregnancy have been extensively investigated in both experimental and clinical studies (5–8). These studies have suggested that hyperglycemia is the major teratogenic factor in diabetic pregnancy (9, 10) and the degree of severity of congenital malformations depends on the glycemic control during the peri-conception period and the first trimester, in particular during the first seven weeks of pregnancy (11, 12). Several teratological pathways such as alterations in the polyol metabolism (13) and reactive oxygen species (14, 15) have been shown to be associated with fetal malformations in diabetic pregnancy.

Maternal diabetes has been shown to impair the development and migration of neural crest cells (NCC) which perturb the epithelial mesenchymal transformation (EMT) causing other abnormalities in the developing heart (16). Recently, we have reported that the altered expression of *Bmp4*, *Msx1* and *Pax3* genes involved in the development of cardiac neural crest cells (CNCC) could contribute to the pathogenesis of maternal diabetes-induced congenital heart defects (17). However, the molecular mechanisms by which teratogenicity of hyperglycemia causes cardiac malformations remain undefined.

Vascular endothelial growth factor (VEGF) plays a key role in vasculogenesis and angiogenesis. A number of angiogenic stimuli have been found to induce VEGF expression, such as cytokines, hormones, phorbol esters, oncogenes, transitional metals, iron chelators and hypoxia (18). In addition, VEGF expression is regulated by nitric oxide (NO). The VEGF-mediated angiogenesis requires NO production from activated endothelial nitric oxide synthase

This work was supported by grants from the Biomedical Research Council (BMRC04/1/21/19/340), and Academic Research Funds (R-181-000-075-112 and R-181-000-101-112), National University of Singapore, Singapore.

[1] To whom correspondence should be addressed at Department of Anatomy, Yong Loo Lin School of Medicine, National University Health System, National University of Singapore, MD10, 4 Medical Drive, Singapore 117597, Singapore. E-mail: anttaysw@nus.edu.sg

Received June 4, 2008.
Accepted July 16, 2008.

DOI: 10.3181/0806-RM-186
1535-3702/08/23311-1421$15.00

(eNOS). NO produced by eNOS plays an important role in the regulation of cell growth and apoptosis as well as in vasodilation and antithrombotic actions (19). Cardiomyocytes constitutively express eNOS starting from early embryonic stages and produce NO under normal physiological conditions (20, 21). Although there is evidence that deficiency of eNOS (22) and overexpression of VEGF (23) result in congenital heart defects in mutant and transgenic mice respectively, the role of these genes has not been specifically linked to cardiac malformations in offspring of diabetic mice. Thus, the present study was carried out to analyze if the expressions of eNOS and VEGF genes are altered in the developing heart of the embryos from diabetic mice.

Materials and Methods

Experimental Animals. Diabetes mellitus was induced in 8 week-old female Swiss Albino mice (Laboratory Animals Centre, Singapore) by an intraperitoneal injection of streptozotocin (STZ, 75 mg/kg body weight; Sigma, USA) on three successive days. Only mice with non-fasting blood glucose level exceeding 16 mmol/l were used as experimental diabetic mice. Control mice maintained the normal blood glucose levels (4–6 mmol/l) before and during pregnancy. Timed mating was carried out by placing four female diabetic or control mice with one normal male mouse in a cage overnight. Noon, on the day where a copulation plug was observed, was counted as embryonic day 0.5 (E0.5). On E13.5 (about 60 pairs of somites), pregnant mice were anaesthetized with pentobarbital (50 mg/kg body wt, intraperitoneally) and embryos were collected after Caesarean section. The developmental stage, E13.5 was chosen for this study, as it corresponds to ~6 weeks of human gestation (24, 25), when all 4 chambers of the heart were clearly distinguishable, and the outflow tract (OFT) was evident (17, 26). Embryos with malformations from diabetic mice and normal embryos from non-diabetic mice were used as the experimental and control groups, respectively. A total of 80 pregnant mice (60 diabetic and 20 control) were used for this study. All procedures involving animal handling were in accordance with the guidelines of the Institutional Animal Care and Use Committee (IACUC), National University of Singapore.

H9C2 Cell Line. The H9C2 cell line (rat cardiac myoblast) obtained from the American Type Culture Collection (ATCC) was used in this study. The DMEM for the H9C2 cell line was obtained from Sigma, USA.

Immunohistochemistry. As described previously (17), the cryosections were incubated overnight with rabbit polyclonal VEGF (1:200; Santa Cruz Biotechnology, Santa Cruz, CA) and mouse monoclonal eNOS (1:250; BD Biosciences, San Diego, CA) antisera in PBS containing 0.1% Triton X-100 (PBS-TX). Sections were then washed in PBS and incubated in the anti-rabbit IgG or anti-mouse IgG (1:200; Sigma) for 1 hour at room temperature at 23°C (RT). The sections were subsequently processed using ABC kit (Vector Laboratories, Burlingame, CA, USA) for 1 hour at RT, and reaction products were finally visualized using 3,3-diaminobenzidine tetrahydrochloride (DAB; Sigma, St. Louis, MO) as the substrate. Tissue sections were counterstained by 0.5% methyl green nuclear stain for 10 min, dehydrated by immersion in alcohol and then cleared with xylene before mounting in medium (Permount; Fisher Scientific, Pittsburgh, PA). Control sections were incubated as described above but without the primary antibody. Photomicrographs were taken with a light microscope (Olympus BX51, Olympus, Japan).

Immunofluorescence. Cardiac myoblast cells were fixed with 4% PF in PBS for 15 min at RT and incubated with mouse monoclonal eNOS antiserum (1:100; BD Biosciences, San Diego, CA) in blocking solution for 1 hour at RT. Subsequently, cells were treated with the anti-mouse IgG conjugated with FITC (1:200, Sigma) in PBS for 1 hour at RT and counterstained with DAPI for 5 min. Photoimages of stained cells were captured in a confocal laser scanning microscope equipped with a digital camera (Olympus FV 1000, Japan).

Western Blot Analysis. Developing hearts were dissected out from embryos and homogenized. The tissue homogenates were centrifuged at 14,000 *g* for 15 min and the supernatant was collected. Protein concentrations of the supernatants were determined by the Bradford method using bovine serum albumin (BSA) as a standard (27). Samples of supernatants were denatured at 95°C for 3 min for electrophoresis. SDS-polyacrylamide gel electrophoresis was performed in 10% gel with 5% stacking gel and with 0.25 M Tris-glycine (pH 8.3), as the electrolyte buffer (Mini-Protein II apparatus; Bio-Rad, Hercules, CA). Protein bands were electroblotted for 1 hour onto 0.45 μm polyvinylidene difluoride (PVDF) membranes (Bio-Rad) using a semi-dry transfer apparatus (Bio-Rad). The membranes were blocked for 1 hour at RT with 5% nonfat dried milk powder in Tris-buffered saline (TBS; pH 7.6), then incubated separately with VEGF (1:1000) or eNOS (1:1000) antibodies in a blocking solution overnight at 4°C and subsequently with horseradish peroxidase (HRP) conjugated anti-rabbit IgG for VEGF (1:5000; Amersham Biosciences, Little Chalfont, UK) and HRP-conjugated anti-mouse IgG for eNOS (1:5000; Amersham Biosciences, Little Chalfont, UK). Specific binding was revealed by enhanced chemiluminescence (ECL kit; Amersham Biosciences), according to the manufacturer's instructions. For loading control, the membrane was incubated with monoclonal anti-actin (1:6000; Sigma-Aldrich, St. Louis, MO) antibody in a blocking solution overnight at 4°C and then incubated with secondary antibody HRP conjugated anti-mouse for actin (1:10,000). Precision prestained standards (Bio-Rad) were used as molecular weight markers. X-ray films (Amersham Biosciences) were scanned with a computer-assisted densitometer (model G-710; Bio-Rad)

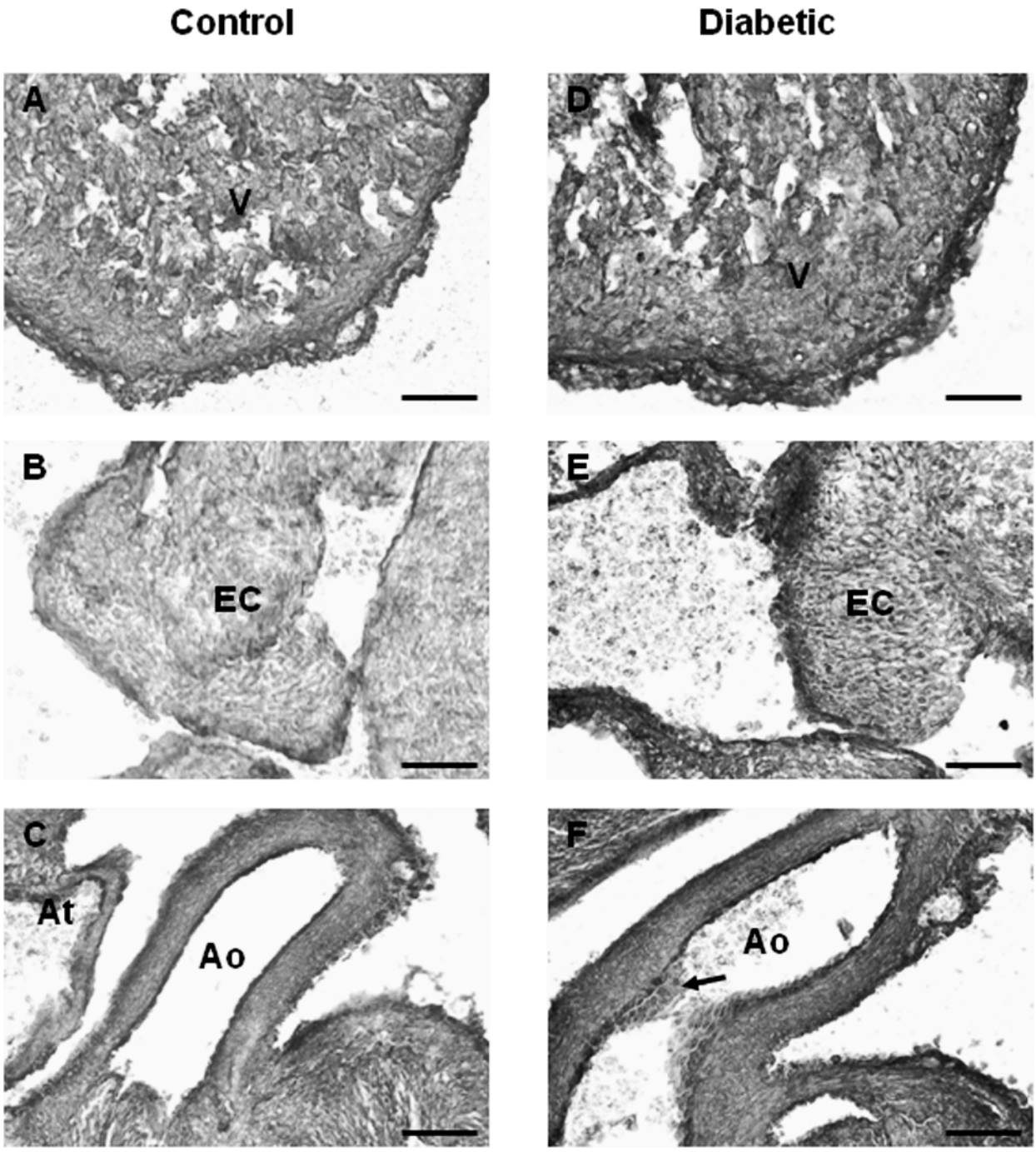

Figure 1. (A–F) Sagittal sections show the immunoreactivity for VEGF in the developing heart of embryos from control and diabetic mice. Compared with control (A–C), the immunoreactivity for VEGF appears to be upregulated in the ventricular myocardium (D), endocardial cells lining the cushion (E), and in the OFT (F) in the embryos from diabetic mice. In addition, embryos from diabetic mice display abnormal vascular endothelium (F: *arrow*). *Bar* A–F 50 μm. At, atrium; Ao, aorta; EC, endocardial cushion; V, ventricle. A color version of this figure is available in the online version of the journal.

to quantify band optical density (Quantity One software; Bio-Rad).

Real-Time Reverse Transcriptase Polymerase Chain Reaction (Real-Time RT-PCR). Total RNA was extracted from the developing hearts of embryos from control and diabetic mice and the cardiac myoblast cells exposed to different glucose concentrations (5.5 mM as control, 33 mM and 44 mM) at different time periods (24 and 48 hours) using the RNeasy mini kit (Qiagen, Valencia, CA). Reverse transcription was performed by adding 2 μg of total RNA to 25 μL of reaction mixture (containing 1× first-strand buffer, 1 U/μL RNasin, 10 mM dNTP mix, and 200 U M-MLV reverse transcriptase; all reagents were purchased from Invitrogen, Carlsbad, CA), which allows

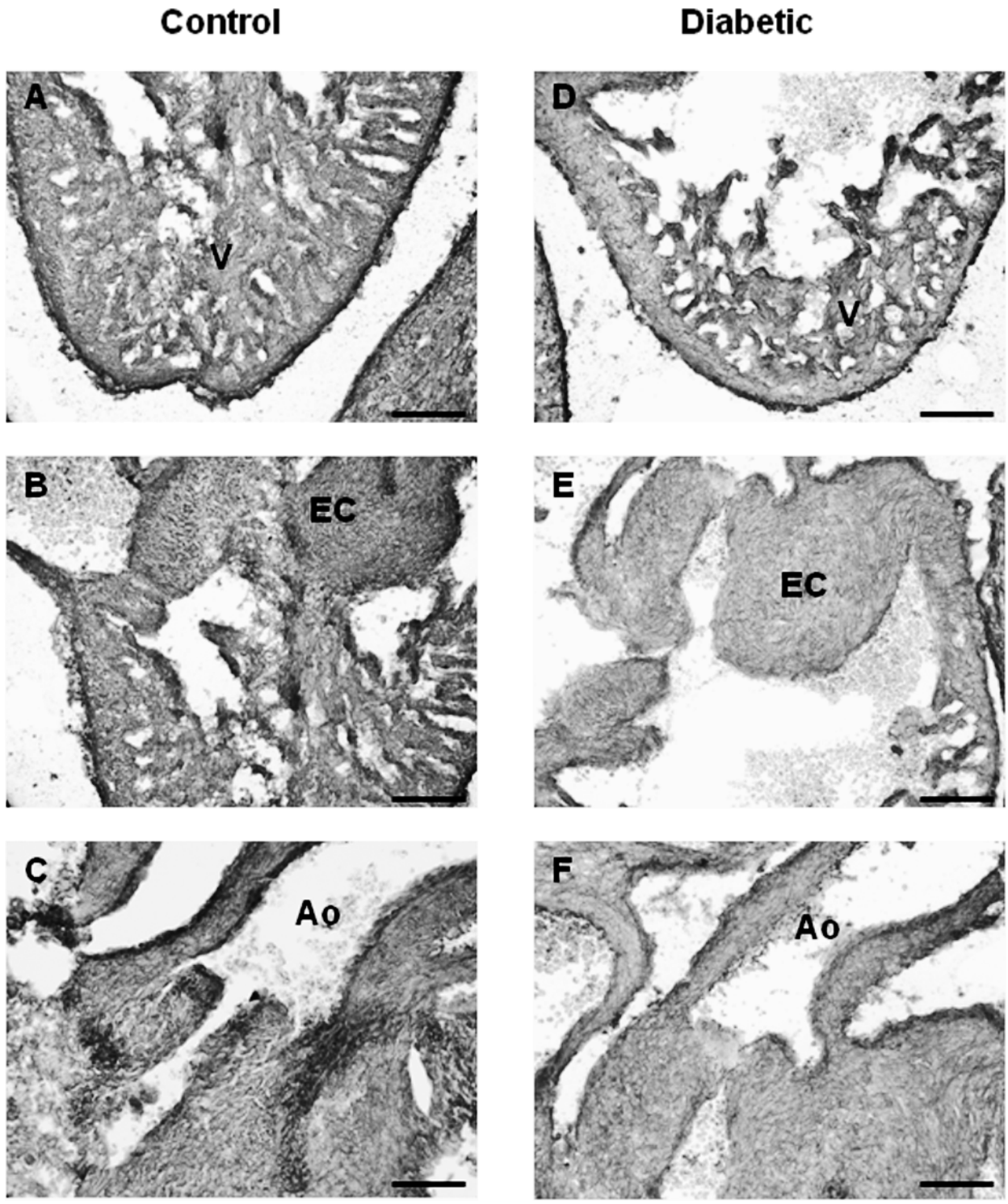

Figure 2. (A–F) Sagittal sections show the immunoreactivity for eNOS in the developing heart of embryos from control and diabetic mice. Compared with control (A–C), the immunoreactivity for eNOS appears to be downregulated in the ventricular myocardium (D), in the cells lining the AV canal and at the surface of cardiomyocytes (E), as well as the cells of the OFT (F) in embryos from diabetic mice. In addition, experimental embryos display thin compact myocardium (D). *Bar* A–F 50 μm. Ao, aorta; EC, endocardial cushion; V, ventricle. A color version of this figure is available in the online version of the journal.

reverse transcription for 50 min at 42°C. The reaction was stopped by heating at 95°C for 5 min and stored at –20°C. Quantitative RT-PCR was performed on a thermocycler using the FastStart DNA Master^{plus} SYBR Green I kit (LightCycler 3, Roche Diagnostics, Indianapolis, IN), according to the manufacturer's instructions. Forward and reverse primer sequences for each gene and their product size are as follows: mouse VEGF (161 bp; forward primer:

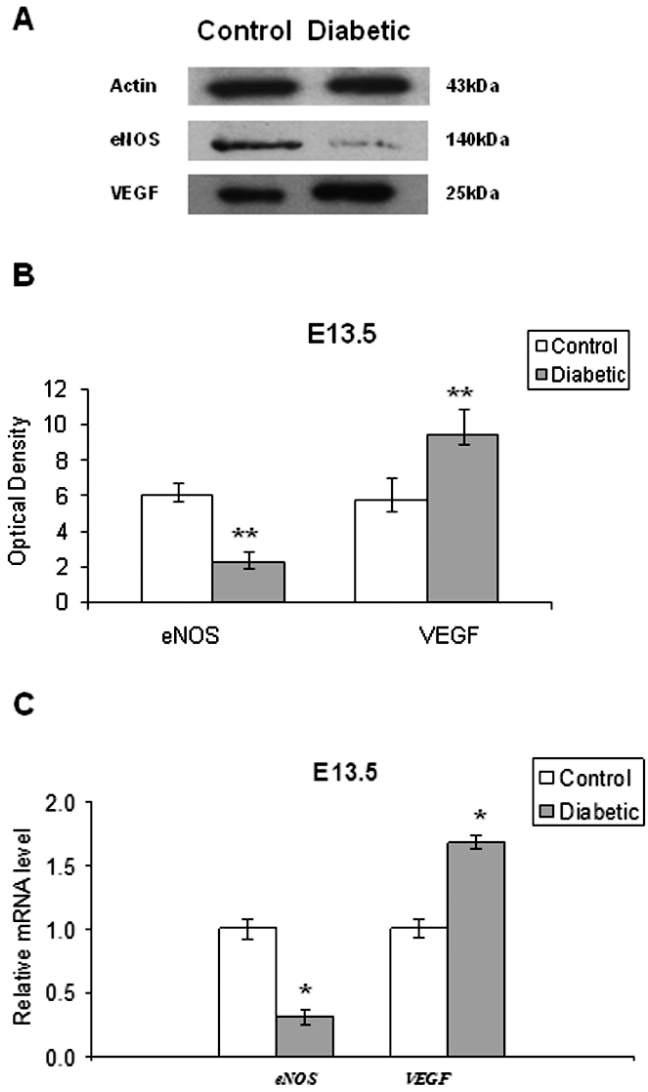

Figure 3. (A, B) Western blot analysis of eNOS and VEGF protein expressions in the developing heart of embryos from control and diabetic mice. (A) β-actin (43 kDa), eNOS (140 kDa) and VEGF (25 kDa) immunoreactive bands. (B) Bar graphs representing eNOS and VEGF show significant changes in the optical density in the developing hearts of embryos from diabetic mice. (C) Real-time RT-PCR analysis of eNOS and VEGF mRNA expression in the developing heart of embryos from control and diabetic mice. Bar graph representing the fold changes of eNOS and VEGF mRNA levels quantified by normalization to the β-actin as an internal control. * $P < 0.05$; ** $P < 0.01$.

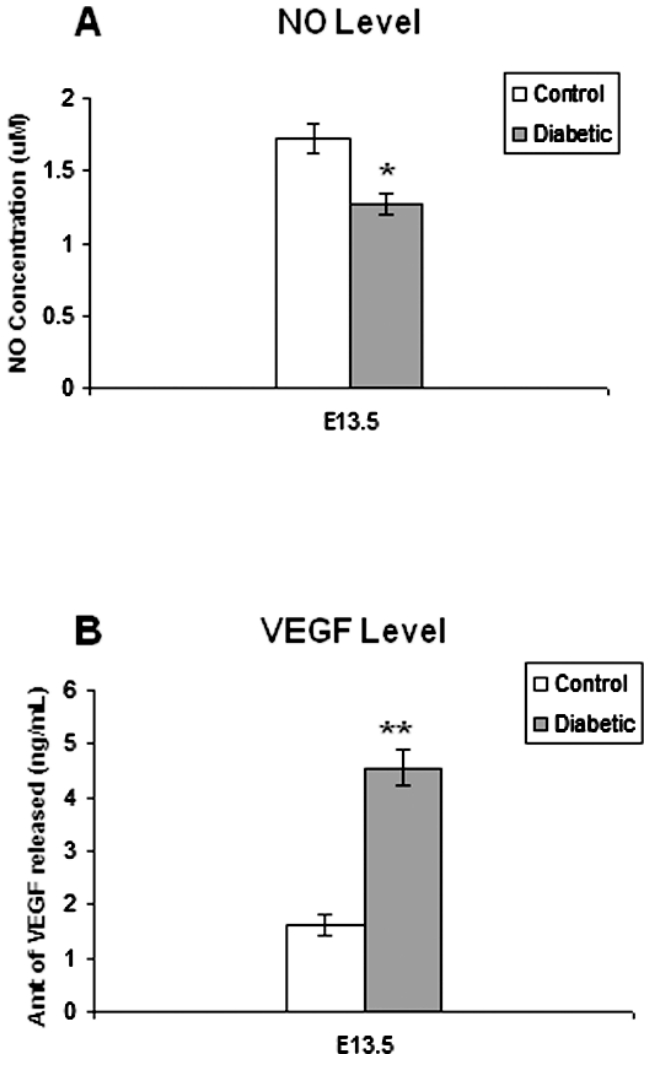

Figure 4. (A) Determination of NO by colorimetric assay in the developing hearts of embryos from control and diabetic mice. NO level is significantly decreased in the developing heart of embryos from diabetic mice. (B) Determination of VEGF by EIA in the developing hearts of embryos from control and diabetic mice. VEGF production is significantly increased in the developing heart of embryos from diabetic mice. * $P < 0.05$; ** $P < 0.01$.

gacttgtgttgggaggagga; reverse primer: cgtgtttctggaagtgagca), mouse eNOS (206 bp; forward primer: gaccctcaccgctacaacat; reverse primer: gccttctgctcattttccag), rat eNOS (243 bp; forward primer: tggcagccctaagacctatg; reverse primer: agtccgaaaatgtcctcgtg), mouse β-actin (165 bp; forward primer: tgttaccaactgggacgaca; reverse primer: ggggtgttgaaggtctcaaa) and rat β-actin (285 bp; forward primer: tcatgaagtgtgacgttgacatccgt; reverse primer: cctagaagcatttgcggtgcaggatg). The RT-PCR was carried out at annealing temperature of 55°C for mouse primers or 60°C

Table 1. The Mean Value in Cells Treated with Different Glucose Concentrations for Varying Time Periods[a]

Glucose concentrations (mM)	Average absorbance			
	24 hours	48 hours	72 hours	96 hours
5.5 (control)	1.02	1.11	1.04	0.91
11	0.97	1.21	1.03	0.89
22	1.20	1.02	1.01	0.95
33	1.04	0.86	0.85	0.69*
44	0.38**	0.35**	0.38**	0.36**

[a] Data represent the mean.
* $P < 0.05$; ** $P < 0.001$ vs corresponding control.

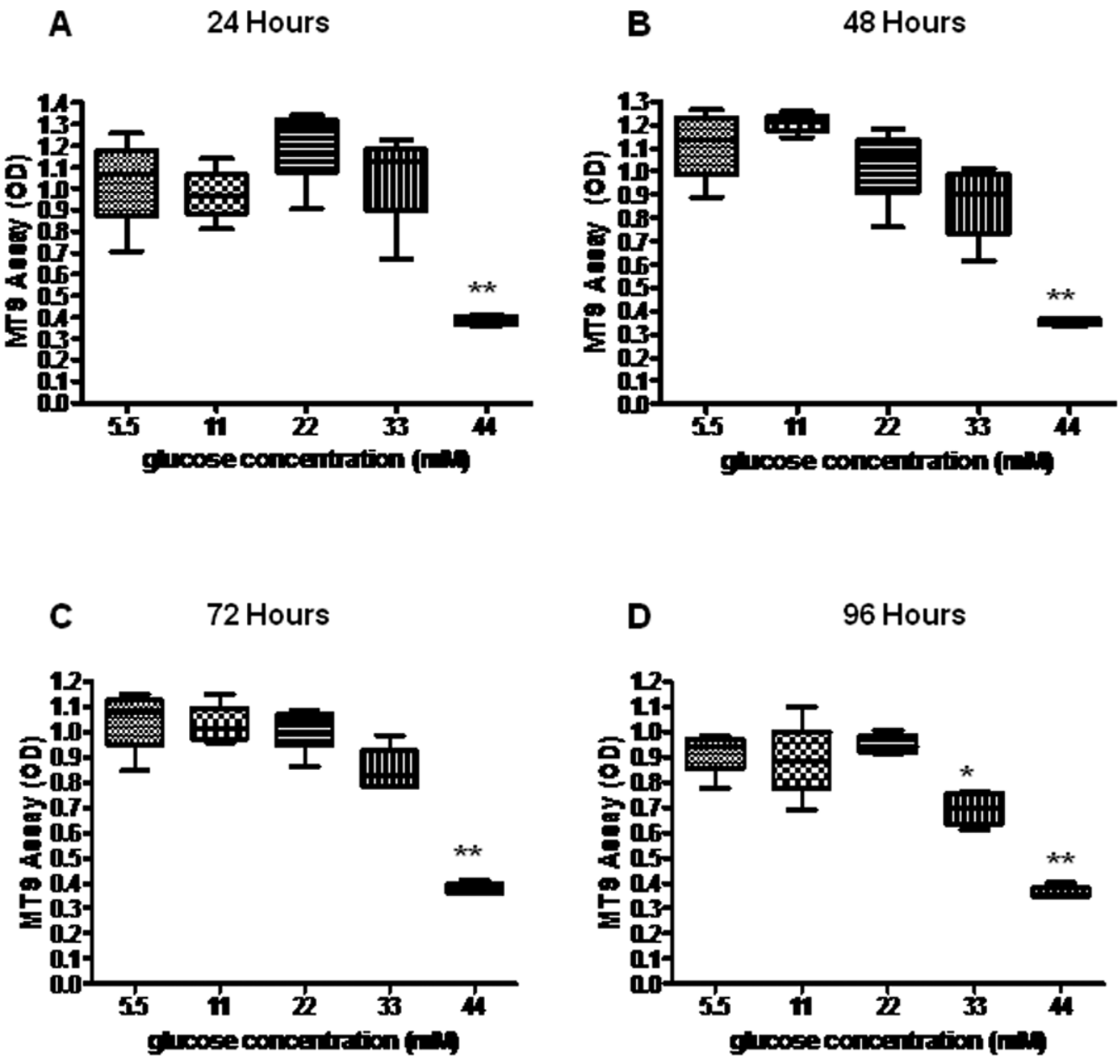

Figure 5. MTS assay show the relative absorbance in cells treated with different concentrations of glucose at 24 hours (A), 48 hours (B), 72 hours (C) and 96 hours (D). Cell viability is significantly decreased in cells treated with 33 mM glucose for 96 hours (D) and 44 mM glucose for all time periods (A–D). * $P < 0.05$; ** $P < 0.001$.

Table 2. Percentage of Cells in Different Phases of the Cell Cycle Treated with Different Glucose Concentrations at 24 Hours and 72 Hours[a]

Glucose concentrations (mM)		Different cell cycle phase analysis			
		Sub-G1 (%)	G0/G1 (%)	S (%)	G2/M (%)
5.5 (control)	24 hours	1.18 ± 0.19	77.63 ± 1.17	6.58 ± 0.75	12.55 ± 0.31
33		1.04 ± 0.03	80.37 ± 0.36	6.04 ± 0.24	10.89 ± 0.13
44		62.18 ± 1.37**	27.15 ± 0.42	4.48 ± 0.30	4.40 ± 0.37
5.5 (control)	72 hours	13.22 ± 0.39	78.90 ± 0.24	2.33 ± 0.14	4.43 ± 0.40
44		98.97 ± 0.15**	0.85 ± 0.11	0.03 ± 0.02	0.02 ± 0.01

[a] Data represent the mean ± SE.
** $P < 0.001$ vs corresponding control.

for rat primers for 45 cycles. The fold change of mRNA was analyzed by the $2^{-\Delta\Delta Ct}$ method (28).

Analysis of Nitric Oxide by Colorimetric Assay. The total amount of nitric oxide (NO) in the heart samples was assessed by the Griess reaction with a colorimetric assay kit (U.S. Biologicals, Swampscott, MA). Hearts from the embryos of diabetic and control mice were homogenized in a homogenizing buffer (T-PER; Pierce Biotechnology, Inc., Rockford, IL) and the supernatant was collected. Eighty μL of each sample was added with 10 μL of enzyme cofactor followed by 10 μL of nitrate reductase and incubated for 4 hours at RT, according to the manufacturer's instructions. Griess reagents (100 μL) were added to the above solution, and the color was allowed to develop for 10 min at RT. The optical density of the samples was measured at 540 nm with a microplate reader (GENios; Tecan Austria GmbH, Grödig/Salzburg, Austria). The nitrite concentration (in micromolar) was determined from a nitrite standard curve.

Analysis of VEGF by Enzyme Immunoabsorbent Assay (EIA). The amount of VEGF concentration in the developing hearts of embryos from control and diabetic mice was determined using the VEGF EIA kit (Chemicon International Inc., Temecula, CA). Fifty μL of supernatant of homogenized heart samples was mixed with 50 μL of diluent, added to the precoated 96-well plate, and incubated with rabbit anti-VEGF antibody for 3 hours at RT. Then, 25 μL of VEGF conjugate was added to each well and incubated for 30 min at RT. After washing with buffer, 50 μL of diluted streptavidin-alkaline phosphatase was added to each well and incubated for 30 min at RT. Subsequently, equal volumes of color reagent A and color reagent B solution were added to each well and kept for 20 min at RT. The optical density was measured at 490 nm. The amount of VEGF (in nanograms per ml) detected in each sample was compared to a VEGF standard curve.

Analysis for Cell Viability. Cell viability was determined by a 3-(4,5-dimethylthiazol-2-yl)-5-(3-carboxymethoxyphenyl)-2-(4-sulfophenyl)-2H-tetrazolium, inner salt (MTS) assay. In a 96-well plate, cells (7×10^3 cells per well) were incubated in 100 μl of DMEM and exposed to different concentrations of glucose for varying time periods. The media were replaced with 20 μl of master mix of MTS in DMEM for 3 hours. The MTS-containing media was collected and absorbance at 490 nm was measured with a microplate reader (GENios firmware).

Cell Cycle Analysis. Cells exposed to different concentrations of glucose for varying time periods were collected by centrifugation and resuspended in 0.5 ml PBS. The cell suspension was added into the 4.5 ml of cold 70% ethanol for overnight at 4°C. Then, 1 ml of cocktail solution (8 ml of PBS, 10 μl of Triton-X, 2 ml of RNase A and 200 μl of propidium iodide, PI) was added into the cell suspension at RT for 30 min. The cell suspension was filtered and transferred into the Dako tubes for flow cytometry analysis using the DAKO machine.

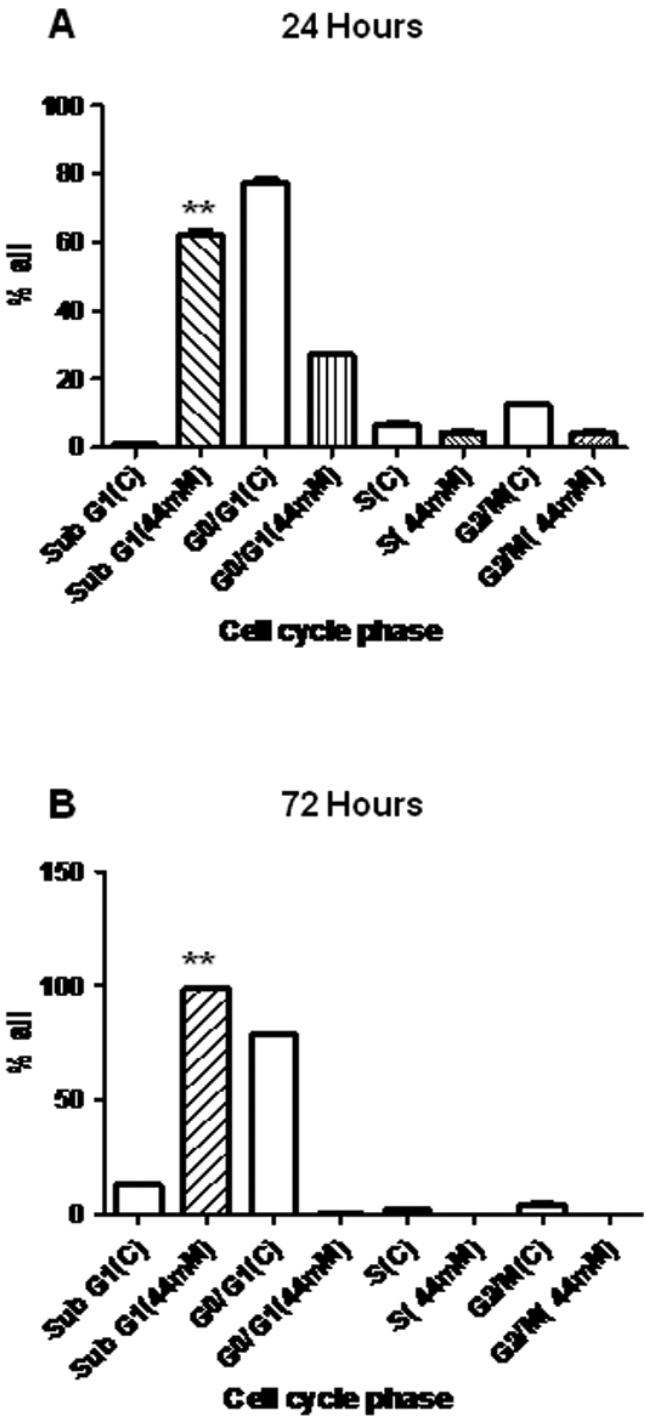

Figure 6. (A, B) Cell cycle analysis show the different phases of the cell cycle treated with 5 mM glucose (control) and 44 mM glucose concentrations at 24 hours and 72 hours. The sub-G1 phase (apoptotic phase) is significantly increased in cells treated with 44 mM glucose concentrations at 24 hours (A) and 72 hours (B). ** $P < 0.001$.

Transmission Electron Microscopy (TEM). Cells were fixed in 2.5% glutaraldehyde in PB at 4°C overnight, osmicated with 1% osmium tetroxide for 1 hour, dehydrated in an ascending series of ethanol and finally embedded in Araldite. Ultrathin sections obtained were double stained

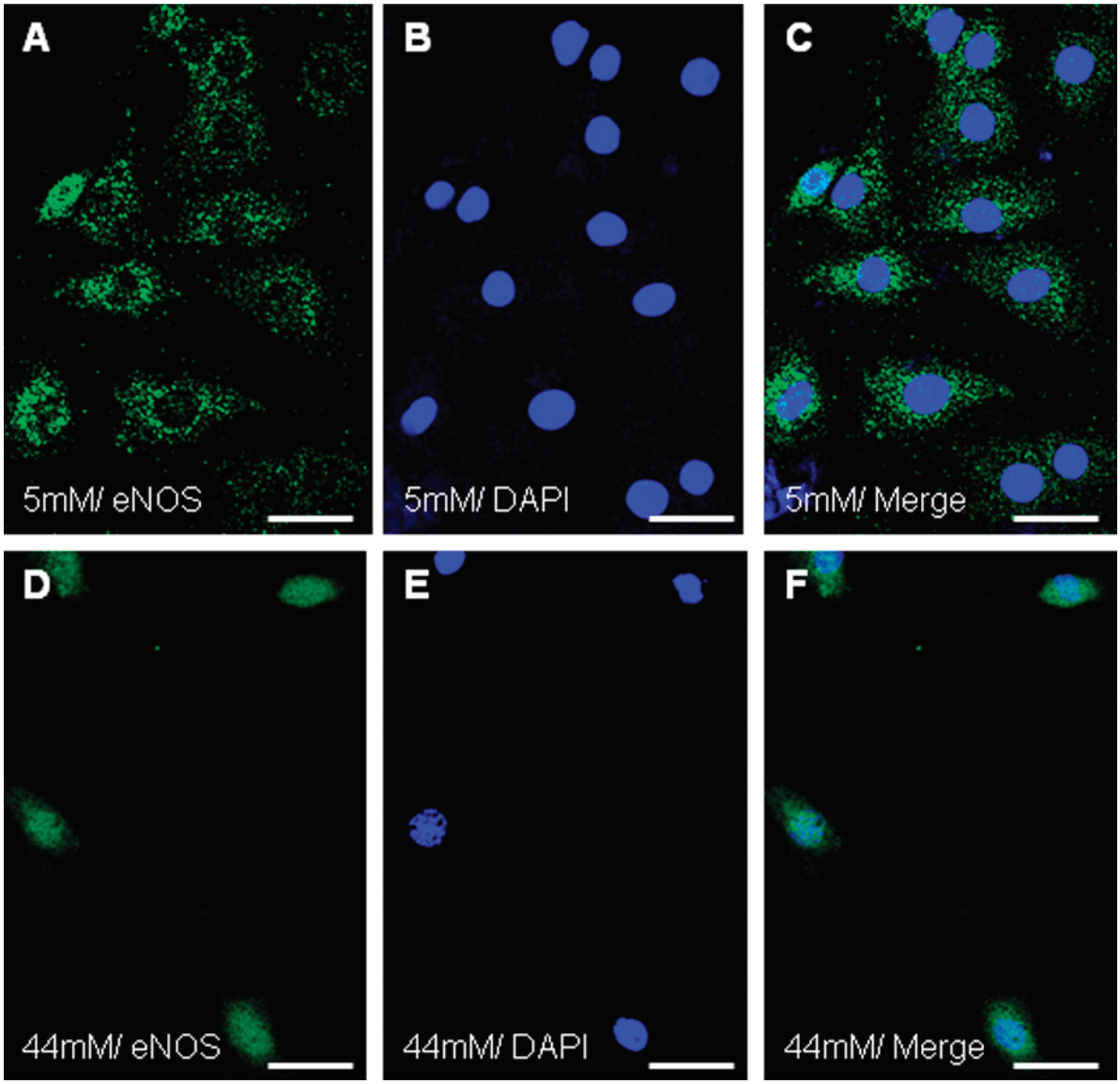

Figure 7. (A–F) The staining of eNOS expression in cells treated with different glucose concentrations at 24 hours. (A-C) Representative cardiac myoblast cells treated with 5 mM glucose (control) concentration. (C) The staining is localized only in the cytoplasm, but not in the nuclei. (D–F) The number of eNOS positive cells appears to be decreased in culture treated with 44 mM glucose concentration when compared to the control culture. (F) The staining is localized in the both cytoplasm and the nuclei of the cells. *Bar* A–F 50 μm.

with lead citrate and uranyl acetate and viewed under a Philips CM120 electron microscope.

Statistical Analysis. Statistical analysis was performed using GraphPad Prism program. The results were analyzed by a two-tailed Student's *t* test to determine the statistical significance of differences between control and experimental samples. For three or more groups, the data were analyzed using one way ANOVA followed by a post hoc Tukey's multiple comparison test. Data are expressed as the mean ± SD. Differences were considered to be statistically significant at $P < 0.05$.

Results

Embryos with malformations from STZ-induced diabetic mice were used in the present study. The number of embryos per litter was significantly decreased ($P < 0.001$) in diabetic mothers (8 ± 1.0) when compared to controls (10 ± 0.5). Embryos (E13.5) obtained from control mice showed clear demarcation of heart chambers and great vessels, whereas embryos of diabetic mice showed a range of cardiac malformations.

In control embryos, VEGF expression was localized to the cells of trabecular layers of myocardium, atrioventricular (AV) canal as well as to the endocardial cells lining the endocardial cushions (EC) and vascular endothelium (Fig. 1A–C). In experimental embryos with cardiac malformations, intense expression of VEGF was localized in the cells lining the OFT, AV canal and mesenchymal cells in the EC

(Fig. 1D–F). The heart appeared to be severely affected showing an aberrant OFT (Fig. 1F), which is characterized by formation of abnormal vascular endothelium, apparently through vasculogenesis. In normal embryos, the eNOS expression was detected in cells lining the AV canal, cardiomyocytes, endothelial cells and the cells of OFT region. eNOS was also expressed in the atria and ventricles (Fig. 2A–C). In contrast, eNOS expression in cardiomyocytes in the ventricular myocardium, the endothelial cells lining the AV canal and the cells of the OFT region appeared to be reduced in embryos of diabetic mice (Fig. 2D–F). Furthermore, the protein and mRNA expression levels of eNOS and VEGF were significantly altered in developing hearts of embryos from diabetic mice, compared to that of controls (Fig. 3A–C).

The total amount of NO in the developing heart of embryos from control and diabetic mice was estimated using a colorimetric assay kit that detects nitrite (NO_2^-), a stable reaction product of NO. The total amounts of NO in the developing heart samples were significantly decreased ($P < 0.05$) in embryos of diabetic mice when compared to that of controls (Fig. 4A). The amount of VEGF produced in the developing heart at E13.5 of control and diabetic mice was determined using Chemikine VEGF EIA kit. Analysis by EIA revealed that VEGF concentration in the developing hearts was significantly increased ($P < 0.01$) in embryos from diabetic mice, when compared with the controls (Fig. 4B).

MTS assay was performed to assess the viability of cells treated with different concentrations of glucose for varying time periods (Table 1; Fig. 5). The cell viability was found to be significantly decreased in culture treated with 33 mM glucose for 96 hours (Table 1; Fig. 5D) and 44 mM glucose at all time periods (Table 1; Fig. 5A–D). Cell cycle analysis showed that about 62% of cells were in subG1 phase at 24 hours of 44 mM glucose concentration (Table 2; Fig. 6A) where as at 72 hours, it was shown that 99% of cells were in subG1 phase (Table 2; Fig. 6B). In contrast, cells treated with 33 mM glucose at 24 hours showed that about 1% of cells were in subG1 phase which was almost similar to the control cells (Table 2).

The number of eNOS positive cells was reduced in culture treated with 44 mM glucose concentration (Fig. 7D–F) when compared to the control culture (Fig. 7A–C) at 24 hours. In addition, the staining was localized in the both cytoplasm and the nuclei of the cells (Fig. 7F). In contrast, the morphology of the cells exposed to 33 mM glucose concentration was very similar to the control cells and the staining was localized only in the cytoplasm, but not in the nuclei (Fig. 7C). In addition, the mRNA expression of eNOS was significantly decreased ($P < 0.001$) in cells treated with 44 mM glucose concentration when compared to the control cells at 24 hours and 48 hours (Fig. 8A). However, there was no significant change in the mRNA expression of eNOS in cells treated with 33 mM glucose concentration when compared to control cells at 24 hours and 48 hours (Fig. 8A).

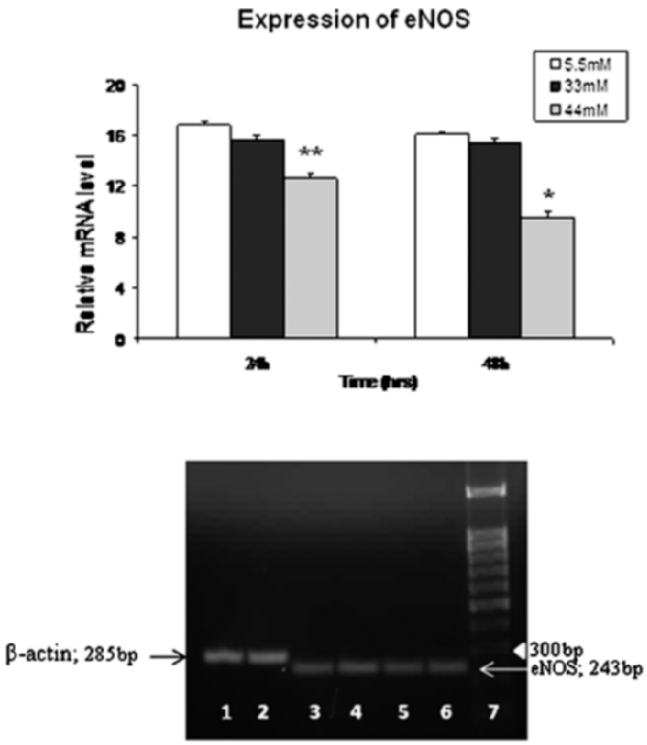

Figure 8. (A) Real-time RT-PCR analysis of eNOS mRNA expression in cells treated with different glucose concentrations at 24 hours and 48 hours. (A) Bar graph representing the fold changes of eNOS mRNA level quantified by normalization to the β-actin as an internal control. (B) The gel electrophoresis shows β-actin (285 bp; lanes 1–2) and eNOS (243 bp; lanes 3–6) genes being amplified. Lane 7: 100-bp DNA ladder. ** $P < 0.001$.

Gel electrophoresis was performed in order to confirm the specific gene being amplified (Fig. 8B).

Ultrastructural study showed that healthy H9C2 cells were large and had normal nuclei (Fig. 9A, B). In contrast, the apoptotic cells had shrunken and became rounded and exhibited margination of nuclear chromatin at the nuclear envelope after treatment with 44 mM glucose concentration for 24 hours. In addition, the nucleus also appeared to be condensed and segregated into several fragments. There were also cell blebbing, aggregation of ribosomes and vacuoles in the cytoplasm (Fig. 9C, D).

Discussion

About 10% of fetuses from diabetic pregnancy display congenital malformations in various organ systems including cardiovascular, gastrointestinal, genitourinary and neurological systems (12, 29). Congenital heart defects involving the ventricular septal defects (VSD) and persistent truncus arteriosus (PTA) are frequently observed in infants of diabetic mothers, but the molecular basis of the defects remain obscure (30). Therefore, the present study was carried out to understand the mechanism of development of cardiac malformations in embryos of diabetic mice.

Maternal diabetes has been shown to induce generalized defects in CNCC development in offspring (16). The

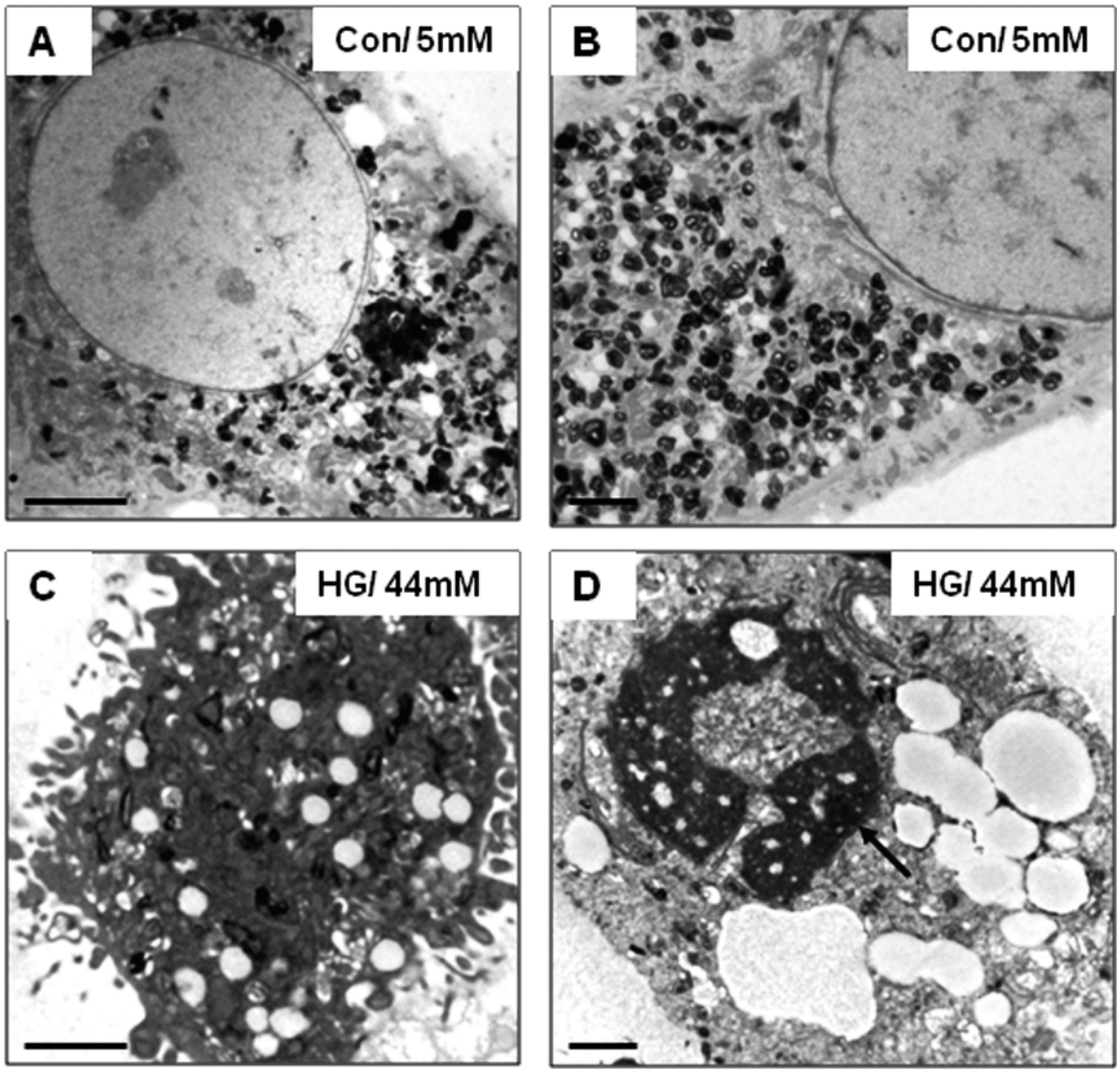

Figure 9. (A–D) Ultrastructural features of cardiac myoblast cells treated with 5.5 mM glucose (control) and 44 mM glucose concentrations at 24 hours. (A, B) Control cells show normal nuclei. (C, D) Cells treated with 44 mM glucose concentration for 24 hours show blebbing, segregation of nucleus, aggregation of ribosomes and vacuoles in the cytoplasm. *Bar* A, C 5 μm; B, D 2 μm.

CNCC play multiple roles during heart development and are particularly essential for OFT development. They are also required for the regulation of proliferation and differentiation of the myocardial cells (31). We have recently reported that maternal diabetes alters the expressions of genes involved in the development of CNCC which could contribute to pathogenesis of congenital heart defects in embryos (17). The morphological phenotype observed in the heart of embryos from diabetic mice appears reminiscent to those seen in the offspring of diabetic mothers (32, 33). The variety of cardiac defects observed in the present study suggests a complex pathogenesis, although several of these abnormalities seem to have resulted from perturbed EMT (34).

Recently, an *in vitro* study has shown that elevation of VEGF by hypoxia blocks the EMT which involves the formation of EC during cardiac development, leading to the cardiac malformations (35). Maintenance of appropriate VEGF levels is required during AV canal morphogenesis (36). Cooper *et al*. (1991) have shown an increase in VEGF production as well as an upregulation of VEGF receptors in diabetic rats (37). Hyperglycemia results in a dramatic upregulation of VEGF expression in a variety of cell types (38, 39), which is due to a transcriptional activation of the VEGF gene (40). The present study showed that maternal diabetes significantly increases the protein and mRNA expressions of VEGF in the developing heart and this upregulation appears to be associated with cardiac malformations observed in embryos from diabetic mice as the embryonic heart development was shown to be disrupted by modest increase in VEGF levels in a transgenic mouse (23). Further, exposure of developing mouse embryos to hyperglycemia has recently been shown to inhibit EMT in culture (41). Atrioventricular septal defects resulting from aberrant

EC formation via EMT defects have also been reported in infants of diabetic mothers (41). Thus, upregulation of VEGF levels in the developing heart of embryos from diabetic mice seems to have deleterious effects on the EC, which is critically dependent on the timing, level and location of altered VEGF expression (42), resulting in cardiac malformations.

During early embryonic heart development, apoptosis occurs in several areas, including AV endocardial cushions, the OFT, AV septum, and trabeculae, as well as papillary muscles of the ventricles (43, 44). It is widely demonstrated that apoptosis is a highly regulated process and increased apoptosis results in cardiac malformations. We have recently reported that cardiomyocyte apoptosis is increased in the heart, including AV endocardial cushion and ventricular myocardium, resulting in congenital heart defects in the embryos of diabetic mice (17). The present study revealed that apoptotic cell death was increased in cardiomyoblasts exposed to the high-glucose concentration *in vitro*. NO produced by eNOS plays an important role in the regulation of cell growth and apoptosis as well as vasodilatation and antithrombotic actions (19). The deficiency in eNOS increases cardiomyocyte apoptosis which results in congenital heart defects during development (22). In the present study, the decreased NO production was associated with downregulation of eNOS in the developing heart of embryos from diabetic mice, indicating the involvement of NO deficiency in the development of cardiac malformations via increased cardiomyocyte apoptosis in diabetic offspring. However, NO has been shown to be pro- or anti-apoptotic on the cellular redox state (45). Further, increased NO was shown to be associated with diabetic embryopathy (46). Hence, further research on the association between cardiac malformations and NO levels may be warranted in diabetic pregnancy.

Cell cycle analysis and viability assay revealed that cell cycle progression and survival of cardiomyocytes are impaired by high glucose concentrations. This could be due to increased cellular oxidative stress as the generation of reactive oxygen species (ROS) was shown to be increased significantly in the cardiac myocytes when exposed to high glucose concentrations (47). ROS formation induces oxidative stress and is associated with caspase-3 activation and apoptosis. Moreover, hyperglycemia-induced ROS has been shown to play a critical triggering role in apoptotic cell death in the diabetic myocardium (48). Results from the present study appear to suggest that high glucose impairs the cell cycle progression and cell viabilities and enhances apoptosis in cardiomyocytes via excessive generation of ROS, forming one of the bases for cardiac malformations as seen in embryos from diabetic mice.

In summary, the present study demonstrated that maternal diabetes induces altered expressions of eNOS and VEGF in the embryos of diabetic mice. Cells treated with high glucose concentrations were found to induce cell death. It is postulated that hyperglycemia may alter the expression of eNOS and VEGF genes that are involved in the regulation of cell growth and vasculogenesis, thereby contributing to cardiac malformations seen in the developing heart of embryos from diabetic mothers. Prevention and treatment of diabetic offspring is a challenging task for clinicians, therefore a thorough analysis study of eNOS and VEGF as potential targets would improve the therapeutic strategies. Further investigations are required to unravel the molecular mechanisms by which hyperglycemia induces oxidative stress and the concomitant perturbed expression patterns of genes of various signaling pathways in the developing heart of embryos from diabetic mothers.

We thank Miss Chan Yee Gek for her technical assistance in electron microscopy work.

1. Hawthorne G, Robson S, Ryall EA, Sen D, Roberts SH, Ward Platt MP. Prospective population based survey of outcome of pregnancy in diabetic women: results of the Northern Diabetic Pregnancy Audit, 1994. BMJ 315:279–281, 1997.
2. Kuhl C, Coustan D, Kitzmiller J, Philipps A, Binder C, Schneider H. Report on the 28th annual meeting of the Diabetic Pregnancy Study Group. Diabetologia 41:suppl 8–14, 1998.
3. Suhonen L, Hiilesmaa V, Teramo K. Glycaemic control during early pregnancy and fetal malformations in women with type I diabetes mellitus. Diabetologia 43:79–82, 2000.
4. Aberg A, Westbom L, Kallen B. Congenital malformations among infants whose mothers had gestational diabetes or preexisting diabetes. Early Hum Dev 61:85–95, 2001.
5. Lazarow A, Kim JN, Wells LJ. Birth weight and fetal mortality in pregnant subdiabetic rats. Diabetes 9:114–117, 1960.
6. Wentzel P, Wentzel CR, Gareskog MB, Eriksson UJ. Induction of embryonic dysmorphogenesis by high glucose concentration, disturbed inositol metabolism, and inhibited protein kinase C activity. Teratology 63:193–201, 2001.
7. Pedersen LM, Tygstrup I, Pedersen J. Congenital malformations in newborn infants of diabetic women. Correlation with maternal diabetic vascular complications. Lancet 1:1124–1126, 1964.
8. Ray JG, O'Brien TE, Chan WS. Preconception care and the risk of congenital anomalies in the offspring of women with diabetes mellitus: a meta-analysis. QJM 94:435–444, 2001.
9. Cockroft DL, Coppola PT. Teratogenic effects of excess glucose on head-fold rat embryos in culture. Teratology 16:141–146, 1977.
10. Ellington SK. In-vivo and in-vitro studies on the effects of maternal fasting during embryonic organogenesis in the rat. J Reprod Fertil 60: 383–388, 1980.
11. Miller E, Hare JW, Cloherty JP, Dunn PJ, Gleason RE, Soeldner JS, Kitzmiller JL. Elevated maternal hemoglobin A1c in early pregnancy and major congenital anomalies in infants of diabetic mothers. N Engl J Med 304:1331–1334, 1981.
12. Mills JL, Baker L, Goldman AS. Malformations in infants of diabetic mothers occur before the seventh gestational week. Implications for treatment. Diabetes 28:292–293, 1979.
13. Baker L, Piddington R, Goldman A, Egler J, Moehring J. Myo-inositol and prostaglandins reverse the glucose inhibition of neural tube fusion in cultured mouse embryos. Diabetologia 33:593–596, 1990.
14. Eriksson UJ, Borg LA. Protection by free oxygen radical scavenging enzymes against glucose-induced embryonic malformations in vitro. Diabetologia 34:325–331, 1991.
15. Eriksson UJ, Borg LA. Diabetes and embryonic malformations. Role of

substrate-induced free-oxygen radical production for dysmorphogenesis in cultured rat embryos. Diabetes 42:411–419, 1993.
16. Eriksson UJ, Cederberg J, Wentzel P. Congenital malformations in offspring of diabetic mothers—animal and human studies. Rev Endocr Metab Disord 4:79–93, 2003.
17. Kumar SD, Dheen ST, Tay SS. Maternal diabetes induces congenital heart defects in mice by altering the expression of genes involved in cardiovascular development. Cardiovasc Diabetol 6:34, 2007.
18. Klagsbrun M, D'Amore PA. Vascular endothelial growth factor and its receptors. Cytokine Growth Factor Rev 7:259–270, 1996.
19. Forstermann U, Closs EI, Pollock JS, Nakane M, Schwarz P, Gath I, Kleinert H. Nitric oxide synthase isozymes. Characterization, purification, molecular cloning, and functions. Hypertension 23:1121–1131, 1994.
20. Balligand JL, Kelly RA, Marsden PA, Smith TW, Michel T. Control of cardiac muscle cell function by an endogenous nitric oxide signaling system. Proc Natl Acad Sci U S A 90:347–351, 1993.
21. Bloch W, Fleischmann BK, Lorke DE, Andressen C, Hops B, Hescheler J, Addicks K. Nitric oxide synthase expression and role during cardiomyogenesis. Cardiovasc Res 43:675–684, 1999.
22. Feng Q, Song W, Lu X, Hamilton JA, Lei M, Peng T, Yee SP. Development of heart failure and congenital septal defects in mice lacking endothelial nitric oxide synthase. Circulation 106:873–879, 2002.
23. Miquerol L, Langille BL, Nagy A. Embryonic development is disrupted by modest increases in vascular endothelial growth factor gene expression. Development 127:3941–3946, 2000.
24. Sissman NJ. Developmental landmarks in cardiac morphogenesis: comparative chronology. Am J Cardiol 25:141–148, 1970.
25. Kaufman MH. The Atlas of Mouse Development. New York: Academic Press, 1992.
26. Srinivasan S, Baldwin HS, Aristizabal O, Kwee L, Labow M, Artman M, Turnbull DH. Noninvasive, in utero imaging of mouse embryonic heart development with 40-MHz echocardiography. Circulation 98: 912–918, 1998.
27. Bradford MM. A rapid and sensitive method for the quantitation of microgram quantities of protein utilizing the principle of protein-dye binding. Anal Biochem 72:248–254, 1976.
28. Livak KJ, Schmittgen TD. Analysis of relative gene expression data using real-time quantitative PCR and the 2(-Delta Delta C(T)) Method. Methods 25:402–408, 2001.
29. Becerra JE, Khoury MJ, Cordero JF, Erickson JD. Diabetes mellitus during pregnancy and the risks for specific birth defects: a population-based case-control study. Pediatrics 85:1–9, 1990.
30. Dinleyici EC, Tekin N, Dinleyici M, Kilic Z, Adapinar B, Aksit MA. Severe fatal course of axial mesodermal dysplasia spectrum associated with complex cardiac defect in an infant of a mother with insulin dependent diabetes. Am J Med Genet A 143:2156–2159, 2007.
31. Schafer K, Neuhaus P, Kruse J, Braun T. The homeobox gene Lbx1 specifies a subpopulation of cardiac neural crest necessary for normal heart development. Circ Res 92:73–80, 2003.
32. Ferencz C, Rubin JD, McCarter RJ, Clark EB. Maternal diabetes and cardiovascular malformations: predominance of double outlet right ventricle and truncus arteriosus. Teratology 41:319–326, 1990.
33. Molin DG, Roest PA, Nordstrand H, Wisse LJ, Poelmann RE, Eriksson UJ, Gittenberger-De Groot AC. Disturbed morphogenesis of cardiac outflow tract and increased rate of aortic arch anomalies in the offspring of diabetic rats. Birth Defects Res A Clin Mol Teratol 70:927–938, 2004.
34. Smoak IW. Hyperglycemia-induced TGFbeta and fibronectin expression in embryonic mouse heart. Dev Dyn 231:179–189, 2004.
35. Natarajan R, Bai W, Lanting L, Gonzales N, Nadler J. Effects of high glucose on vascular endothelial growth factor expression in vascular smooth muscle cells. Am J Physiol 273:H2224–H2231, 1997.
36. Dor Y, Camenisch TD, Itin A, Fishman GI, McDonald JA, Carmeliet P, Keshet E. A novel role for VEGF in endocardial cushion formation and its potential contribution to congenital heart defects. Development 128: 1531–1538, 2001.
37. Cooper RG, Taylor CM, Choo JJ, Weiss JB. Elevated endothelial-cell-stimulating angiogenic factor activity in rodent glycolytic skeletal muscles. Clin Sci (Lond) 81:267–270, 1991.
38. Taniyama Y, Morishita R, Hiraoka K, Aoki M, Nakagami H, Yamasaki K, Matsumoto K, Nakamura T, Kaneda Y, Ogihara T. Therapeutic angiogenesis induced by human hepatocyte growth factor gene in rat diabetic hind limb ischemia model: molecular mechanisms of delayed angiogenesis in diabetes. Circulation 104:2344–2350, 2001.
39. Williams B, Gallacher B, Patel H, Orme C. Glucose-induced protein kinase C activation regulates vascular permeability factor mRNA expression and peptide production by human vascular smooth muscle cells in vitro. Diabetes 46:1497–1503, 1997.
40. Roguin A, Nitecki S, Rubinstein I, Nevo E, Avivi A, Levy NS, Abassi ZA, Sabo E, Lache O, Frank M, Hoffman A, Levy AP. Vascular endothelial growth factor (VEGF) fails to improve blood flow and to promote collateralization in a diabetic mouse ischemic hindlimb model. Cardiovasc Diabetol 2:18, 2003.
41. Enciso JM, Gratzinger D, Camenisch TD, Canosa S, Pinter E, Madri JA. Elevated glucose inhibits VEGF-A-mediated endocardial cushion formation: modulation by PECAM-1 and MMP-2. J Cell Biol 160:605–615, 2003.
42. Hallaq H, Pinter E, Enciso J, McGrath J, Zeiss C, Brueckner M, Madri J, Jacobs HC, Wilson CM, Vasavada H, Jiang X, Bogue CW. A null mutation of Hhex results in abnormal cardiac development, defective vasculogenesis and elevated Vegfa levels. Development 131:5197–5209, 2004.
43. Watanabe M, Choudhry A, Berlan M, Singal A, Siwik E, Mohr S, Fisher SA. Developmental remodeling and shortening of the cardiac outflow tract involves myocyte programmed cell death. Development 125:3809–3820, 1998.
44. Abdelwahid E, Pelliniemi LJ, Niinikoski H, Simell O, Tuominen J, Rahkonen O, Jokinen E. Apoptosis in the pattern formation of the ventricular wall during mouse heart organogenesis. Anat Rec 256:208–217, 1999.
45. Brune B. The intimate relation between nitric oxide and superoxide in apoptosis and cell survival. Antioxid Redox Signal 7:497–507, 2005.
46. Ornoy A. Embryonic oxidative stress as a mechanism of teratogenesis with special emphasis on diabetic embryopathy. Reprod Toxicol 24:31–41, 2007.
47. Cai L, Li W, Wang G, Guo L, Jiang Y, Kang YJ. Hyperglycemia-induced apoptosis in mouse myocardium: mitochondrial cytochrome C-mediated caspase-3 activation pathway. Diabetes 51:1938–1948, 2002.
48. Kajstura J, Fiordaliso F, Andreoli AM, Li B, Chimenti S, Medow MS, Limana F, Nadal-Ginard B, Leri A, Anversa P. IGF-1 overexpression inhibits the development of diabetic cardiomyopathy and angiotensin II-mediated oxidative stress. Diabetes 50:1414–1424, 2001.